Structures and Spectroscopic Properties of Gold(I) Complexes of 1,3,5-Triaza-7-phosphaadamantane (TPA). 2. Multiple-State Emission from (TPA)AuX (X = Cl, Br, I) Complexes†

Zerihun Assefa, Brian G. McBurnett, Richard J. Staples, and John P. Fackler, Jr.*

Department of Chemistry and Laboratory for Molecular Structure and Bonding, Texas A&M University, College Station, Texas 77843

Received March 3, 1995®

Temperature-dependent photoluminescence (PL) and structural studies of (TPA)AuBr, **2**, (TPA)AuI, **3**, and [(TPAH)AuI][AuI_2], **4**, are reported. Unlike (TPA)AuCl, **1**, compound **2** has two emission bands with relative intensities which depend upon the excitation wavelength used. Upon excitation at 320 nm, a strong orange emission centering at 647 nm is observed. Changing the excitation wavelength to 340 nm results in the observance of only a bright white, structured emission centering ca. 450 nm. Each of the two emission bands shows a distinct excitation spectrum, suggesting poor coupling between the excited states responsible for the emissions. Compared to that of **2**, the LE band of **3** is blue-shifted to 617 nm, whereas the structured HE band is unshifted at ca. 450 nm. The relative intensity of the LE band to the HE band decreases (with no shift in energy) when the excitation wavelength is changed from 320 to 350 nm. Similar to those of **2**, the emission bands of **3** also are sensitive to the excitation energy. The HE bands of both **2** and **3** are short lived (<10 ns) whereas the LE bands have lifetimes of 0.8 and 2.7 μs, respectively. On the basis of these observations, the complexes appear to show multiple emitting states in their solid state structures. The systematic changes occurring with variation of the halide X and the lifetime data suggest that the LE band originates from a triplet metal-centered transition (^{3}MC). The HE emission band appears to originate from a halide to metal charge transfer (^{1}XMCT) excited state. Protonation of the ligand TPA significantly alters the PL properties of the complexes in accord with changes in the Au···Au separation. The metal-centered LE band of the protonated complex (TPAHBr)AuBr, **2P**, is observed at the blue-shifted position of 587 nm when compared to that of **2**. Protonation of **3** with 0.1 N HCl produces **4**. Compound **4** luminesces strongly with emission maxima at 655 nm at 78 K. A simple model that correlates the LE emission with the Au···Au separation has been developed. The Au···Au separations in these species are predicted from the position of the emission energy using the equation $(E + P)/r$ = constant, where E is the emission energy, P is the singlet−triplet separation, and r corresponds to the Au···Au distance. The result is supported by extended Hückel MO calculations where, upon shortening of the Au···Au separation, the HOMO (σ_u) orbital destabilizes and causes a decrease in the HOMO−LUMO gap. Crystal data: [(TPAH)AuI][AuI_2], **4**, orthorhombic, *Pnma* (No. 62) with a = 15.453(3) Å, b = 11.050(2) Å, c = 9.113(2) Å, V = 1556.1(5) Å^3, Z = 4, R = 0.0419, R_w = 0.0548.

Introduction

One of the intriguing phenomena in gold(I) complexes is the frequent observance of a weak metal−metal interaction in the solid state.[1] Association of gold(I) complexes through aurophilic interactions has been observed in neutral, anionic, and cationic anionic systems.[2−4] Relativistic effects that result in the expansion of the 5d and contraction of the 6s orbitals have been suggested[5] as the principal cause for the enhancement of the metal−metal interaction. An interesting physical property exhibited by most gold(I) compounds with close Au···Au contacts[4] is the visible luminescence observed under UV excitation. Not surprisingly, the luminescence has been associated with an Au···Au interaction that is thought to lead to a metal-centered, MC, emission.[6] Recently,[7] however, three-coordinate mononuclear gold(I) complexes were also found which strongly luminesce.

While examples of luminescent gold(I) complexes with short Au···Au contacts are abundant,[6] the literature to date contains few emitting mononuclear gold(I) compounds,[7] although trigo-

* Author to whom correspondence should be addressed.

† Part 1 of this series is ref 10.

® Abstract published in *Advance ACS Abstracts,* September 1, 1995.

(1) Puddephatt, R. J. *The Chemistry of Gold*; Elsevier: Amsterdam, 1978.

(2) (a) Wells, A. F. *Structural Inorganic Chemistry*, 5th ed.; Clarendon Press: Oxford, U.K., 1987. (b) Schmidbaur, H. Organogold Compounds. *Gmelin Handbook of Inorganic Chemistry*; Springer-Verlag: Berlin, 1980.

(3) (a) Jones, P. G. *Gold Bull.* **1981**, *14*, 102. (b) Jones, P. G. *Gold Bull.* **1986**, *19*, 46. (c) Schmidbaur, H. *Angew. Chem., Int. Ed. Engl.* **1976**, *15*, 728. (d) Schmidbaur, H. *Gold Bull.* **1990**, *23*, 11.

(4) (a) Hall, K. P.; Mingos, D. M. *Prog. Inorg. Chem.* **1984**, *32*, 237. (b) Jones, P. G. *Gold Bull.* **1981**, *14*, 102−118, 159−166; **1983**, *16*, 114−124; **1986**, *19*, 46−57. (c) Uson, R.; Laguna, A. *Coord. Chem. Rev.* **1986**, *70*, 1. (d) Khan, M. N. I.; King, C.; Heinrich, D. D.; Fackler, J. P., Jr.; Porter, L. C. *Inorg. Chem.* **1989**, *28*, 2150. (e) Khan, M. N. I.; Fackler, J. P., Jr.; King, C.; Wang, J. C.; Wang, S. *Inorg. Chem.* **1988**, *27*, 1672. (f) Schmidbaur, H.; Graf, W.; Müller, G. *Angew. Chem., Int. Ed. Engl.* **1988**, 23. (g) Khan, M. N. I.; Wang, S.; Fackler, J. P., Jr. *Inorg. Chem.* **1989**, *28*, 3588. (h) Vogler, A.; Kunkley, H. *Chem. Phys. Lett.* **1988**, *150*, 135.

(5) (a) Pyykkö, P.; Desclaux, J.-P. *Acc. Chem. Res.* **1979**, *12*, 276. (b) Pitzer, K. S. *Acc. Chem. Res.* **1979**, *12*, 271. (c) Jansen, M. *Angew. Chem., Int. Ed. Engl.* **1987**, *26*, 1098. (d) Mehrotra, P.; Hoffmann, R. *Inorg. Chem.* **1978**, *17*, 2187. (e) Jiang, Y.; Alvarez, S.; Hoffmann, R. *Inorg. Chem.* **1985**, *24*, 749. (f) Dedieu, A.; Hoffmann, R. *J. Am. Chem. Soc.* **1978**, *100*, 2074.

(6) (a) Ludwig. W.; Meyer, W. *Helv. Chim. Acta* **1982**, *65*, 934. (b) Jaw, H.-R. C.; Savas, M. M.; Rogers, R. D.; Mason, W. R. *Inorg. Chem.* **1989**, *28*, 1028. (c) King, C.; Wang, J.-C.; Khan, M. N. I.; Fackler, J. P., Jr. *Inorg. Chem.* **1989**, *28*, 2145.

(7) (a) King, C.; Khan, M. N. I.; Staples, R. J.; Fackler, J. P., Jr. *Inorg. Chem.* **1992**, *31*, 3236. (b) MaCleskey, T. M.; Gray, H. B. *Inorg. Chem.* **1992**, *31*, 1733.

0020-1669/95/1334-4965$09.00/0

nally coordinated phosphine species generally may emit. In these three-coordinate phosphine species, the luminescence has been assigned[7] to a metal-centered $p_z \rightarrow d_\sigma$ phosphorescence. Other possible transition modes such as ligand centered, LC, or ligand to metal charge transfer, LMCT, are also observed depending upon the types of ligands present.[8,9] A recent report by the Bruces on dithiol[8a] complexes and our own ongoing investigation of sulfur systems[8b] indicate that a LMCT transition dominates the emission in these gold(I)−sulfur ligand complexes. We recently reported the first example of emission arising from a LC transition in some bis(phosphine)gold(I) xanthate complexes.[9] The neutral TPA−gold halides,[10] LAuX, have a dimer of "crossed lollypops" molecular structure. The small cone angle[11] of the phosphine ligand allows a short intermolecular Au···Au contact in the solid state. The aurophilic Au···Au interaction is significantly altered upon protonation of a ligand nitrogen atom. A remarkable shift in the emission energy occurs which was found to correlate with the change in the Au···Au distance.[10]

Continuing our studies of TPA−gold complexes, this paper reports detailed photoluminescence results on (TPA)AuX (X = Cl^-, Br^-, I^-) and the related [(TPAH)AuI](AuI_2), **4**. The luminescence observed in these complexes has been examined as a function of temperature and excitation wavelength in order to elucidate the nature of the excited state responsible for the emission. These complexes appear to possess a rarely observed[12] multiple-state emission that originates from excited states having two different (MC and LMCT) orbital parentages. To the best of our knowledge this is the first time that multiple-state emission has been reported in gold(I) photochemistry. Preliminary observations suggest that other crossed dimer complexes of gold(I) with ligands such as those which coordinate through S atoms also may display this behavior.

Experimental Section

General Details. All experiments with the unprotonated TPA ligand and its compounds were routinely carried out under pure dry nitrogen using a standard Schlenk apparatus. Solvents were purified prior to use. Water was deionized and doubly distilled. The TPA ligand was prepared by following literature procedures.[10,13−14] The compounds (TPA)AuCl, **1**, (TPAHCl)AuCl, **1P**, and (TPA)AuI, **3**, were prepared as reported earlier.[10,15]

Synthesis of (1,3,5-Triaza-7-phosphaadamantane)gold(I) Bromide (TPA)AuBr·CH_3CN, 2. Compound **2** was synthesized by modifying the previously reported procedure.[10] To a stirred suspension of (THT)AuCl (40 mg, 0.125 mmol) in 10 mL of CH_2Cl_2 was added the TPA ligand (19.6 mg, 0.125 mmol) at once and the solution stirred for 1 h. The solvent was removed by vacuum pump suction, and the white product was suspended in 10 mL of CH_3CN. To the suspension was added KBr (14.9 mg, 0.125 mmol), and the solution was stirred for 3 h. After filtration, the solvent was reduced *in vacuo* and Et_2O was added to precipitate the white solid. Single crystals for X-ray structural determination as well as for the PL studies were grown by slow diffusion of hexane into a CH_3CN solution of the complex.

Dissolving **2** in 0.1 N HBr and slowly evaporating the aqueous solution provided the protonated complex, P-(1,3,5-triaza-7-phosphaadamantane hydrobromide)gold(I) bromide, **2P**, (TPAHBr)AuBr, mp 220 °C dec. Anal. Calcd for $C_6H_{13}N_3PBr_2Au·0.5H_2O$ (523.84): C, 13.75; H, 2.67; N, 8.02; Br, 30.51. Found: C, 12.23; H, 3.02; N, 7.88; Br, 30.88.

Synthesis of P-(1,3,5-Triaza-7-phosphaadamantane)gold(I) Iodide Diiodoauride(I), [(TPAH)AuI][AuI_2], 4. Compound **4** initially was synthesized unexpectedly in the attempt to protonate **3**. After **3** was dissolved in 0.1 N HCl and any remaining suspension was filtered off, the clear solution was left for a slow evaporation at room temperature. Decomposition to gold metal was observed after several days. However, small quantities of light yellow crystals of **4** suitable for X-ray and luminescence work were obtained. The crystals showed a strong red emission even at room temperature, and thus, no attempt was made to grow large crystals. Using 0.1 N HI instead of HCl also provided **4** with no evidence of decomposition to gold metal, mp 214 °C dec.

Structural Studies. The structure of **4** was determined with data collected on a Nicolet R3m/E diffractometer (SHELXTL 5.1) by employing Mo Kα radiation (λ = 0.710 73). A light yellow block-shaped crystal, 0.3 × 0.2 × 0.1 mm, was mounted on a glass fiber with epoxy cement at room temperature. The unit cell constants were determined from 25 machine-centered reflections. Intensities of all reflections with 2θ values 4−55° were measured by the ω-scanning technique. The structure factors were obtained after Lorentz and polarization corrections. Empirical absorption corrections based on azimuthal (ψ) scans of reflections were applied. The crystal data are presented in Table 1.

Table 1. Crystal Data for [Au(TPAH)I][AuI_2]

formula	$C_6H_{13}N_3PI_3Au_2$
fw	932.701
space group	*Pnma* (No. 62)
a, Å	15.453(3)
b, Å	11.050(2)
c, Å	9.113(2)
V, Å^3	1556.1(5)
Z	4
d_{calc}, g/cm^3	3.977
μ(Mo Kα), mm^{-1}	24.778
radiation (λ, Å)	graphite monochromated Mo Kα (0.710 73)
temp, K	293
transm factor: max, min	0.999, 0.281
R,[a] R_w[b]	0.0419, 0.0548

[a] $R = \sum||F_o| - |F_c||/\sum|F_o|$. [b] $R_w = \{[\sum w(|F_o| - |F_c|)^2]/[\sum w(F_o)^2]\}^{1/2}$; $w^{-1} = [\sigma^2(|F_o|) + g|F_o|^2]$.

Cell constant changes as a function of temperature were used to calculate the Au···Au separations at various temperatures different from that of the data collection. No evidence of phase change was observed with any of the crystals.

Spectroscopic Studies. UV−vis studies were carried out on a Cary 17 spectrophotometer. Spectral grade acetonitrile and doubly distilled, deionized H_2O were used in the spectrophotometric studies. Emission and excitation spectra were recorded on an SLM AMINCO Model 8100 spectrofluorometer using a xenon lamp as the excitation source. Data are presented in Table 2. Both emission and excitation spectra are corrected for instrumental responses. The excitation radiation for the

(8) (a) Jones, W. B.; Yuan, J.; Narayanaswamy, R.; Young, M. A.; Elder, R. C.; Bruce, A. E.; Bruce, M. R. M. *Inorg. Chem.* **1995**, *34*, 1996. A preprint of this paper has been gratefully received. (b) Assefa, Z.; Staples, R. J.; Fackler, J. P., Jr. In preparation.
(9) Assefa, Z.; Staples, R. J.; Fackler, J. P., Jr. *Inorg. Chem.* **1994**, *33*, 2790.
(10) Assefa, Z.; McBurnett, G. B.; Staples, R. J.; Fackler, J. P., Jr.; Assman, B.; Angermaier, K.; Schmidbaur, H. *Inorg. Chem.* **1995**, *34*, 75.
(11) Darensbourg, M. Y.; Daigle, D. *Inorg. Chem.* **1975**, *14*, 1217.
(12) (a) Hager, C. D.; Crosby, G. A. *J. Am. Chem. Soc.* **1975**, *97*, 7031. (b) Glazen, M. M.; Lees, A. *J. Am. Chem. Soc.* **1989**, *111*, 6602. (c) Zuleta, J. A.; Bevilacqua, J. M.; Rehm, J. M.; Eisenberg, R. *Inorg. Chem.* **1992**, *31*, 1332. (d) Zuleta, J. A.; Bevilacqua, J. M.; Proserpio, D. M.; Harvey, P. D.; Eisenberg, R. *Inorg. Chem.* **1992**, *31*, 2396. (e) Zuleta, J. A.; Chesta, C. A.; Eisenberg, R. *J. Am. Chem. Soc.* **1989**, *111*, 8916. (f) Eitel, E.; Oelkrug, D.; Hiller, W.; Strähle, J. *Z. Naturforsch.* **1980**, *35b*, 1247.
(13) (a) Delerno, J. R. Trefonas, L. M.; Darensbourg, M. Y.; Majeste, R. J. *Inorg. Chem.* **1976**, *15*, 516. (b) Darensbourg, D. J.; Joo. F.; Kannisto, M.; Katho, A. *Organometallics* **1992**, *11*, 1990.
(14) (a) Alyea, E. C.; Fisher, K. J.; Johnson, S. *Can. J. Chem.* **1989**, *67*, 1319. (b) Fisher, K. J.; Aleyea, E. C.; Shahnazarian, N. *Phosphorus, Sulfur Silicon* **1990**, *48*, 37.
(15) Growing a crystal of (TPA)AuCl from $C_2H_4Cl_2$ produces an entirely different structure with no solvent in the lattice: space group $R\bar{3}$, R = 0.0283, a = 22.586(2) Å, c = 9.813(2) Å, V = 4335(1) Å^3. This material has an extended-chain structure with equal Au···Au distances of 3.394(2) Å, not the dimer[10] structure of **1**·CH_3CN. The optical properties of the extended-chain material also are different from those of **1**·CH_3CN and will be reported elsewhere.

Table 2. Observed Excitation and Emission Data for the Gold(I) Complexes of TPA with the Observed Au···Au separations

compd	λ_{ex}, nm	temp, K	λ_{em}, nm	Au···Au, Å
1	290	78	674	
		200	656	3.092
		250	645	
		298	643	
1P	290	78	596	
		200	588	3.303
		250	586	
		298	582	3.322
2	320	78	647	
		200	638	3.089
		298	633	3.107
	340	78*	~450* (421, 430, 438, 448, 457, 468, 477)	
2P	295	78	580	
		298	580	
	325	78	~491* (467, 491, 518)	
3	320	78	617	
		298	614	
	350	78	617, ~450* (421, 428, 434, 448, 456, 465, 477, 486)	
4	330	78	655	
		200	655	2.916
		298	652	2.92

solid samples was filtered through a 0.1 M KNO_2 solution to reduce scattered light. Low-temperature measurements were conducted on a cryogenic setup of local design. Crycon grease and a drop of collodion were used to attach the compounds (crystal and powder, respectively) to the sample holder. Crycon grease and collodion alone were scanned both at low and room temperatures and showed no emission in the region of interest. In all of the PL experiments, both the emission and excitation slit widths were kept at 2 nm or less. Various baths (acetone/dry ice (200 K), CCl_4/N_2 (250 K)) were used to control the sample temperature above 78 K.

MO Calculations. Extended Hückel, EH, calculations were performed on a Macintosh IIfx computer using the molecular modeling CAChe software package.[16] Energy minimization was conducted using the MM2 program, which is included in the CAChe software, prior to running the EH calculation. The Au−P and the Au−X distances were fixed at the values found from the crystal structure. The orbital energy and exponent parameters used in the EH calculation were obtained from Pyykkö's work and correspond to relativistic values.[17] For p and d orbitals the weighted average of the low and high angular momentum values were used to satisfy the CAChe criteria. For the two-coordinate complexes idealized $C_{\infty v}$ and $D_{\infty h}$ symmetries were assumed.

Results

Luminescence Studies. Compound 2, (TPA)AuBr·CH_3CN. The temperature-dependent emission spectra of a single crystal of **2** are shown in Figures 1 and 2. When the sample is excited at 320 nm or less, a broad, low-energy, LE, emission, Figure 1, is observed at 647 nm (78 K). The emission maximum of the band blue-shifts slightly with a temperature increase. At 200 K (λ^{ex}_{max} = 320 nm) the band blue-shifts by ca. 200 cm^{-1} and is observed at 638 nm. Further temperature increase to room temperature blue-shifts the emission band by ca. 320 cm^{-1} when compared to that of the 78 K spectrum.

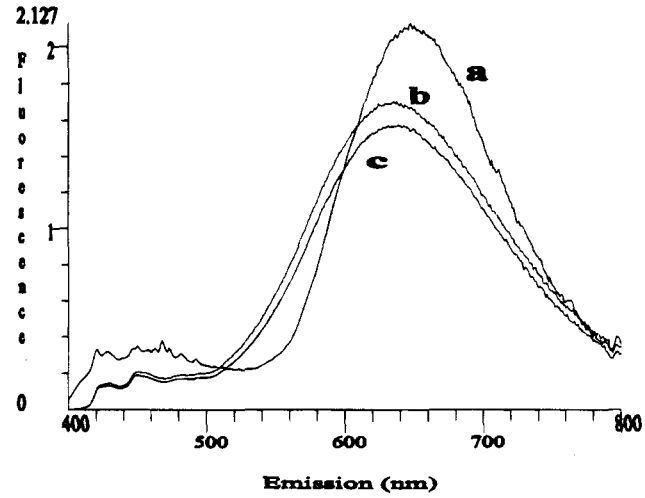

Figure 1. 1. Temperature-dependent emission spectra of the LE band of **2** at (a) 78, (b) 200, and (c) 298 K excited at 320 nm.

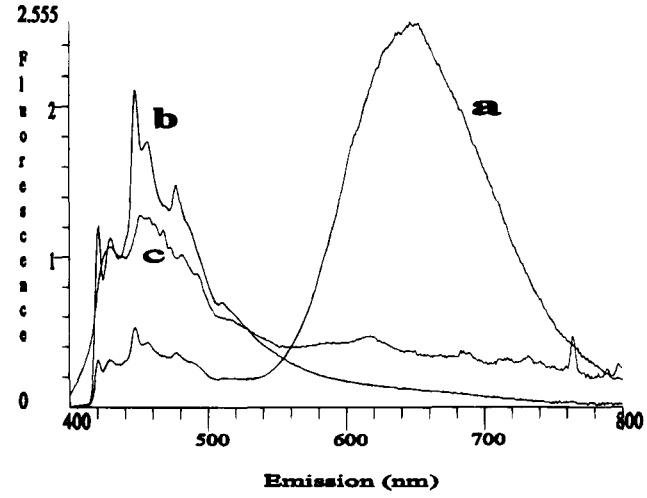

Figure 2. Dependence of the emission spectra of **2** on excitation wavelength: (a) excited at 320 nm at 78 K; (b) excited at 340 nm at 78 K; (c) excited at 340 nm at 298 K. The small differences observed between part a in Figure 1 and part a in Figure 2 reflect variances in different runs.

In addition to the LE band, the luminescence spectrum of **2** contains an intense, structured, high-energy, HE, band centering at ca. 450 nm. The intensity of the HE band shows a strong dependence on the excitation wavelength. This dependence of the HE emission band on the excitation wavelength is shown in Figure 2. At the excitation wavelength of 320 nm (Figure 2a), the emission from the HE band is weak and the LE emission dominates. However, when the excitation wavelength is changed to 340 nm (Figure 2b,c) the LE band is quenched and only the bright blue HE emission is observed at 78 K. Increasing the temperature does not cause any significant change in the spectral profile except that the vibronic components are less well resolved at higher temperatures. The vibronic components of the HE band are observed at 421, 430, 438, 448, 457, 468, and 477 nm, with a spacing around 450 ± 50 cm^{-1} (Table 2). However, no clear progressions emerge.

Each of the two emission bands in **2** has a distinct excitation spectrum. In Figure 3, the excitation spectra obtained by monitoring the HE and LE emission bands are compared. The excitation spectrum corresponding to the HE band (monitored at 450 nm) displays a band that maximizes at ca. 340 nm whereas the LE band shows an excitation spectrum that rises steeply at about 325 nm with increasing energy and is present throughout the UV (Figure 3a). Excitation at shorter wave-

(16) *CAChe (Computer Aided Chemistry)*; CAChe Scientific, Inc., TEKTRONIX Co.: Beaverton, OR 97077.
(17) (a) Pyykkö, P. *Chem. Rev.* **1988**, *88*, 563. (b) Pyykkö, P. In *Methods In Computational Chemistry*; Wilson, S., Ed.; Plenum Press: New York, 1988; Vol. 2, pp 137−221. (c) Pyykkö, P.; Lohr, L. L. *Inorg. Chem.* **1981**, *20*, 1950. (d) Mehrotra, P.; Hoffmann. R. *Inorg. Chem.* **1978**, *17*, 2187. (e) Jiang, Y.; Alvarez, S.; Hoffmann, R. *Inorg. Chem.* **1985**, *24*, 749.
(18) Pyykkö, P.; Li, J.; Runeberg, N. *Chem. Phys. Lett.*, in press.

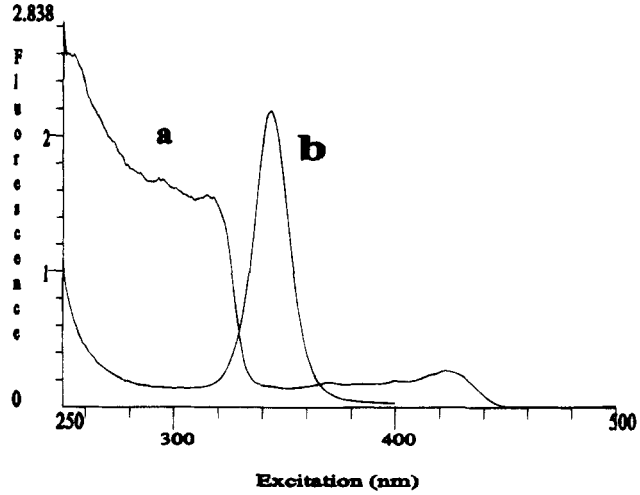

Figure 3. Excitation spectra of **2** monitored at the LE and HE emission bands: (a) monitored at 647 nm; (b) monitored at 450 nm.

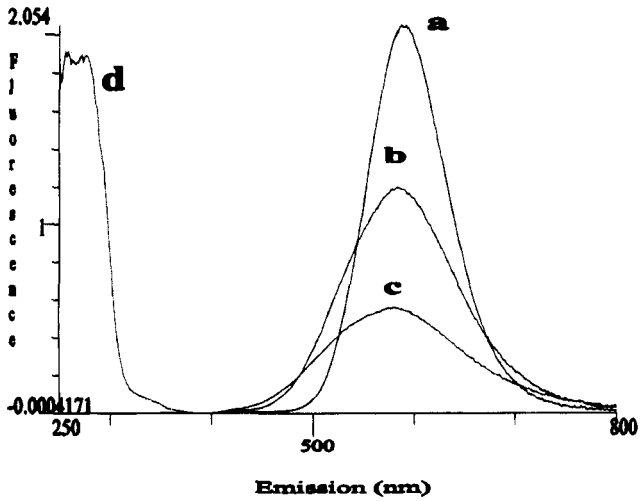

Figure 4. Temperature-dependent emission spectra of **2P**: (a) 78 K excited at 290 nm; (b) 298 K excited at 290 nm; (c) 78 K excited at 340 nm. Trace d is the excitation spectrum at 78 K.

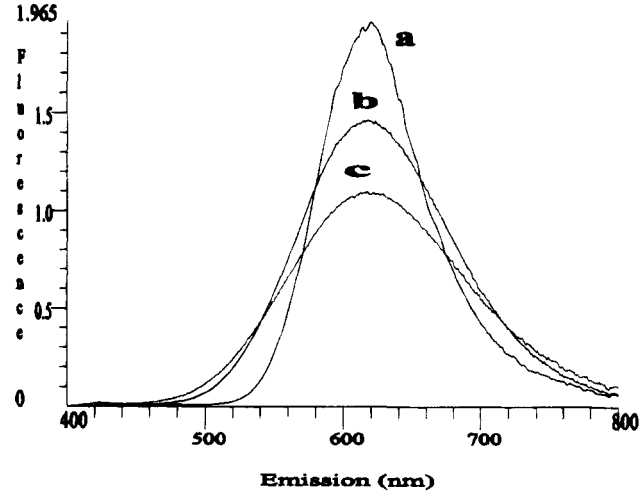

Figure 5. Temperature-dependent emission spectra of the LE band of **3** at (a) 78, (b) 200, and (c) 298 K excited at 320 nm.

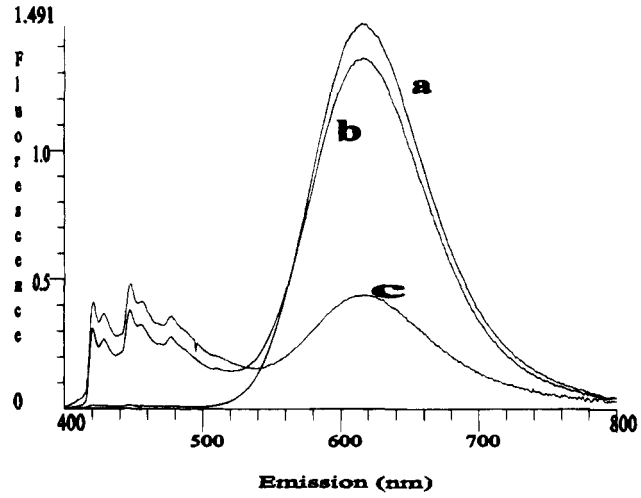

Figure 6. Dependence of the emission spectra of **3** on excitation wavelength: (a) excited at 320 nm at 78 K; (b) excited at 340 nm at 78 K; (c) excited at 350 nm at 78 K.

lengths than 320 nm does not lead to any significant emission from the HE excited state. Protonation of **2** with HBr to form (TPAHBr)AuBr·0.5H_2O, **2P**, alters the emission spectrum significantly. At 78 K the intense red-orange (647 nm) LE band of **2** blue-shifts by ca. 1600 cm^{-1} in **2P** and an intense yellow emission (Figure 4) is observed centered at 587 nm (λ^{ex}_{max} = 290 nm). Compared to **2**, the emission band profile in **2P** is unsymmetrical at the high-energy side of the spectrum. The emission band in **2P** blue-shifts by ca. 230 cm^{-1} upon a temperature increase to room temperature (579 nm at 298 K). The excitation profiles of the two complexes are also different. Compared to that of **2**, the excitation spectrum of **2P** is significantly blue-shifted and maximizes at ca. 290 nm (320 nm for **2**).

Compound 3, (TPA)AuI. Figure 5 presents the temperature-dependent LE luminescence spectra of **3**. The features are similar to those observed for **2**. At 78 K, compound **3** displays two emission bands, Figure 6, with relative intensities which depend significantly on the excitation wavelength. For excitation at 320 nm, a fairly broad asymmetrical LE band is observed (Figure 5a) at 617 nm at 78 K. Compared to that of **2**, this LE emission band in **3** is blue-shifted by 752 cm^{-1} (at 78 K). With a temperature increase, the intensity of this band decreases and becomes broader and more asymmetrical. Between 78 and 298 K (λ_{ex} = 320 nm) the emission intensity drops nearly by half and the peak position of the band slightly blue-shifts.

When the excitation wavelength is changed from 320 to 340 nm, the emission intensity of the LE band (617 nm) decreases, Figure 6b, and the structured HE band appears at ca. 450 nm (ca. in a 1:3 ratio). The peak maxima, Table 5, appear to have an energy spacing which is less than that observed for **2**, appearing around 380 ± 50 cm^{-1} (Table 2), but there is no obvious progression. Changing the excitation wavelength to 350 nm significantly reduces the intensity of the LE emission, Figure 6c, and its ratio to the HE band becomes ca. 1:1.

In Figure 7, the excitation spectra of **3** monitored at the two emission bands are compared. Similar to the situation in **2**, the HE emission band in **3** has a nearly symmetrical and a relatively narrow excitation band at (λ^{ex}_{max} = 340 nm) at 78 K. The LE emission band, on the other hand, shows a broad excitation band at λ^{ex}_{max} = 324 nm with a tail which extends up to ca. 360 nm and then levels off. Even though there exists an overlap region, the LE and HE bands show distinctively different excitation spectra, indicating poor coupling between the two excited states. These PL studies clearly indicate that the two excited states that lead to emission in these complexes are populated mainly by direct excitation and very little excitation transfer occurs between these states.

Compound 4, [(TPAH)AuI][AuI_2]. Figure 8 presents the temperature-dependent emission spectra of **4**. Single crystals of **4** luminesce intense red at room temperature from a broad emission band centering at 655 nm. Unlike the compounds

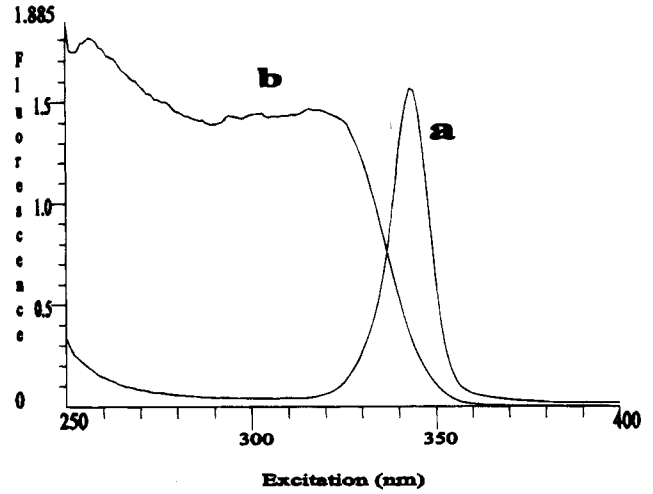

Figure 7. Excitation spectra of **3** monitored at the LE and HE emission bands: (a) monitored at 617 nm; (b) monitored at 450 nm.

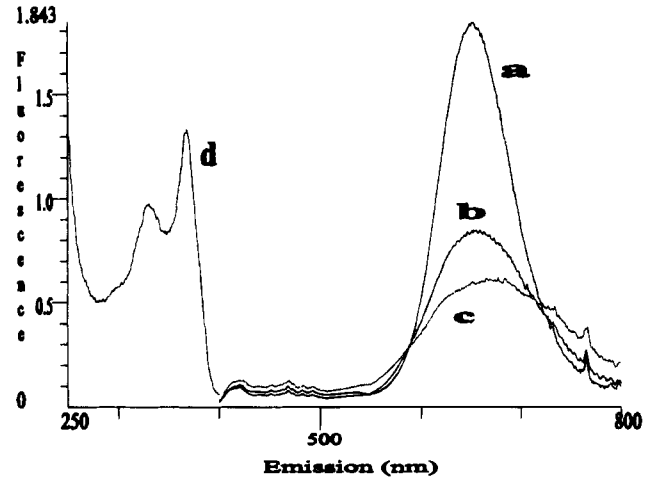

Figure 8. Temperature-dependent emission spectra of **4** at (a) 78, (b) 200, and (c) 298 K. Trace d is the excitation spectrum at 78K.

Table 3. Lifetime Data for the HE and LE Emission Bands of the TPA-Gold(I) Complexes

compd	LE band, μs	HE band, ns
(TPA)AuCl (**1**)	0.76, 11.3	
(TPAHCl)AuCl (**1P**)	1.19, 3.75	
(TPA)AuBr (**2**)	0.885	3.1
(TPA)AuI (**3**)	2.7	<10

described above, the blue shift in the emission band as the temperature is increased in **4** is small (only ca. 3 nm between 78 and 298 K). However, a broadening of the band with a temperature increase is evident. The excitation spectrum, monitored at 655 nm, shows bands at 330 and 368 nm. Both excitation bands lead to the single LE emission at 655 nm.

Lifetimes. The room-temperature lifetime data of **1**, **1P**, **2**, and **3** are compared in Table 3. For the LE emission band, the samples were excited with the 265 nm laser line whereas the 356 nm line was used for the HE emission. While the decay curve of the LE bands for **2** and **3** were satisfactorily fit by a single-exponential equation, the profiles of **1** and **1P** required two exponentials to fit the data. In all the complexes, the LE emission bands show lifetimes in the microsecond region.

The decay profile of the HE emission band of **2** was measured at 450 nm using the 356 nm laser line. After deconvolution of the excitation source, a short lifetime of ca. 3 ns was obtained from the decay curve. The decay profile of the HE band of **3** was also measured similarly. Unfortunately, sample decomposition did not allow a prolonged exposure to the laser light. As a result, our ability to collect several measurements for better averaging was limited. However, this emission clearly decays very fast, with a lifetime of <10 ns.

Table 4. Atomic Coordinates ($\times 10^4$) and Equivalent Isotropic Displacement Parameters ($Å^2 \times 10^3$) for [Au(TPAH)I][AuI_2], **4**[a]

	x	*y*	*z*	*U*(eq)[b]
Au(1)	2846(1)	2500	4408(1)	36(1)
Au(2)	1925(1)	2500	1610(1)	39(1)
I(1)	4370(1)	2500	3252(1)	46(1)
I(2)	1859(1)	4783(1)	1356(1)	56(1)
P(1)	1584(3)	2500	5621(5)	34(1)
N(1)	851(10)	2500	8361(14)	33(4)
N(2)	76(8)	3607(12)	6448(11)	51(4)
C(1)	1700(11)	2500	7635(16)	33(5)
C(2)	833(9)	3774(13)	5443(13)	46(4)
C(3)	−406(15)	2500	6164(22)	66(9)
C(4)	326(10)	3633(13)	7965(14)	51(5)

[a] Estimated standard deviations are given in parentheses. [b] Equivalent isotropic *U* defined as one-third of the trace of the orthogonalized U_{ij} tensor.

Table 5. Selected Bond Lengths (Å) and Angles (deg) for [Au(TPAH)I][AuI_2], **4**[a]

Au(1)−Au(2)	2.920(1)	Au(1)−I(1)	2.579(2)
Au(1)−P(1)	2.242(5)	Au(2)−I(2)	2.535(1)
Au(2)−I(2A)	2.535(1)		
Au(2)−Au(1)−I(1)	95.1(1)	Au(2)−Au(1)−P(1)	90.4(1)
I(1)−Au(1)−P(1)	174.6(1)	Au(1)−Au(2)−I(2)	95.7(1)
Au(1)−Au(2)−I(2A)	95.7(1)	I(2)−Au(2)−I(2A)	168.6(1)
Au(1)−P(1)−C(1)	114.0(6)	Au(1)−P(1)−C(2)	120.5(4)
		Au(1)−P(1)−C(2A)	120.5(4)

[a] Estimated standard deviations are given in parentheses.

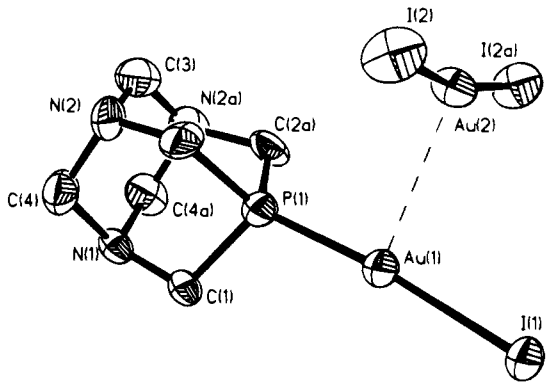

Figure 9. Thermal ellipsoid drawing of **4** with 50% probability.

Structures. The structures of **1**, **1P**, and **2** have been reported.[10] Compound **4** crystallizes in the orthorhombic system, and the space group is *Pnma* (No. 62). Pertinent crystallographic data are given in Table 1. Table 4 lists the positional and thermal parameters of **4**, and the selected bond distances and angles are given in Table 5. The thermal ellipsoid drawing of **4** is shown in Figure 9. There are two different Au atoms in the asymmetric unit. One of the Au atoms coordinates to two iodides with an I(2)−Au(2)−I(2A) angle of 168.6(1)°. The Au−I distances are identical by symmetry, 2.535(1) Å. The other Au atom coordinates to the TPAH and iodide ligands. The Au(1)−P(1) distance is 2.242(5) Å. The Au(1)−I(1) distance, 2.579(2) Å, is slightly longer than the Au(2)−I(2) distance. The TPAH ligand is protonated at one of the nitrogen atoms (N(1)). The AuI_2^- ion interacts with $[(TPAH)AuI]^+$ in a very nearly perpendicular geometry. The iodides on AuI_2^- are only 3.52 Å from another gold(I) atom in a $[(TPAH)AuI]^+$ unit. The Au···Au distance, 2.920(1) Å, between $[(TPAH)AuI]_2^-$ and AuI_2^- is the shortest found to date in the crossed dimers of

the TPA system we have been investigating. Thus there is a fairly strong auriophilic metal−metal interaction in this system. The geometry around the Au(1) atom deviates from linearity, giving a P(1)−Au(1)−I(1) angle of 174.6°. The Au−P distance, 2.242 Å, is slightly longer than that in (TPA)AuCl (2.221 Å).

Table 2 shows the small effect a change of temperature has on the Au···Au separation for compounds **1P**, **2**, and **4**. The Au···Au distance in **1P** changes from 3.322 to 3.303 Å when the temperature is decreased from 298 to 200 K. Both the Au−Cl and the Au−P distances also decrease slightly as the temperature decreases from ambient to 200 K (2.294 and 2.221 Å at 298 K to 2.287 and 2.214 Å at 200 K, respectively). Similarly, the Au···Au distance in **2** also decreases slightly with a temperature decrease while the Au−Cl and Au−P distances remain unchanged. In **4**, the Au···Au separation of 2.92 Å (298 K) decreases slightly at 200 K and becomes 2.916 Å (200 K). The change in the Au···Au separation with temperature, as determined from the cell constant changes as a function of temperature, is the smallest decrease observed in this series of compounds so far investigated.

Discussion

Nature of the LE Emission Band. The solid state emission spectra of the unprotonated (TPA)AuX (X = Cl^-, Br^-, I^-) depend on the ligand X. All of the complexes show an intense LE red emission in the 600−700 nm region. The luminescence properties of **1** have been reported previously,[10] where the LE emission band appears at 674 nm at 78 K. A comparison of the emission spectra of the three compounds (**1**−**3**) indicates that, at a given temperature, the LE emission band blue-shifts as the softness of the halide X increases (674, 647, and 617 nm for X = Cl, Br and I, respectively at 78 K). On going from **1** to **2**, the emission band blue-shifts by 620 cm^{-1}. Compared to that of **1**, the blue shift of **3** is 1370 cm^{-1}. In addition, a temperature increase has been found to blue-shift the emission band in all of the compounds. Moreover, a shift of the LE emission has also been observed when the TPA ligand is protonated. In both **1** and **2**, protonation blue-shifts the emission bands by nearly the same amount (1900 and 1600 cm^{-1}, respectively).

The LE band previously has been correlated with an Au···Au interaction observed in the solid state. Protonation of the TPA ligand has been shown to increase the Au···Au separation in **1P**. As a result of the reduced Au···Au interaction a blue shift in the luminescence spectra of the (TPAHCl)AuCl complex has been observed. A similar blue shifting with an increased Au···Au separation has been observed in other Au(I) systems.[19] The large Stokes shift between the excitation and emission bands ($>1.6 \times 10^4$ cm^{-1}) is indicative of a large distortion in the excited state (compared to the ground state) and suggests that the emission is phosphorescence. Lifetime measurements conducted on the compounds (Table 3) confirm that the LE band is a phosphorescence. As suggested previously[10] for **1**, the LE bands of both **2** and **3** are assigned to a phosphorescent emission originating from a metal centered (MC) $d_{z^2} \rightarrow p_z$ transition.

Luminescence Energy vs Au···Au Interaction. An early attempt by Fackler et al. to correlate the luminescence energy with the Au···Au separation in dinuclear gold(I) systems failed to provide any consistency.[6c] Recently, Bruce et al.[8a] examined neutral dinuclear dithiol complexes for such properties and also concluded that no correlation exists between the Au···Au distance and the emission energy. In their system, the lowest emission was assigned to LMCT. The Au···Au interaction cannot be expected to have a systematic influence on the energies of the frontier orbitals responsible for the emission in these systems involving LMCT.

On the other hand, a recent theoretical study by Pyykkö showed[18] that the auriophilic Au···Au interaction in the perpendicular model systems, $[(PH_3)AuX]_2$, increases as the softness of the ligand X increases. Since the (TPA)AuX compounds crystallize out as crossed "lollypop or torch" dimers and show short Au···Au contacts, they are ideal model compounds to further delineate the general rules governing the supramolecular association of gold(I) complexes through auriophilic interaction. The temperature-dependent luminescence and crystallographic studies as well as systematic ligand variation and protonation experiments reported here relate directly to the theoretical predictions made by Pyykkö. In the atomic spectrum of the Au^+ ion, the energy difference[20] between the singlet $^1S_0$ ground state and the singlet excited state $^1D_2$ is 29 620 cm^{-1}. Below the lowest singlet excited state there are three triplet states, $^3D_1$, $^3D_2$, and $^3D_3$, at energies of 27 764, 17 639, and 15 039 cm^{-1}, respectively. According to Kasha's rule,[21] emission is expected to originate from the lowest $^3D_3$ state. The LE emission observed for the compounds reported here occurs roughly at this latter energy. In the spectrum of the Au^+ ion, the separation between the lowest singlet and the lowest triplet excited states is 14 581 cm^{-1}, a much larger[20] splitting than found for the copper(I) or silver(I) gas-phase ions.

As discussed earlier, the Au···Au interaction[10] which is present in the dimers has been implicated as the source for the LE emission of the complexes studied in this work. Thus it was our strong expectation that a dependence of the LE emission energy on the Au···Au distance would be observed. Several factors influence the Au···Au distance in these compounds, including protonation of the TPA ligand, the temperature, and the particular halide ligand. These factors have provided the opportunity to change the Au···Au distance in various ways and study the subsequent spectroscopy. When the Au···Au distance is varied either by protonation of the TPA ligand or by a change in the temperature, the position of the LE emission shifts in a manner that reflects a change in the HOMO−LUMO gap. In each of the compounds studied, lengthening of the Au···Au distance through protonation or thermal expansion has been found to blue-shift the emission energy. Protonation of the TPA ligand has a direct pronounced influence on the Au···Au distance. For example, in **1**, protonation lengthens the Au···Au distance by 0.211 Å (3.092 Å vs 3.303 Å for **1** and **1P** at 200 K, respectively). As a result, the emission energy blue-shifts by ca. 1900 cm^{-1} (674 and 596 nm for **1** and **1P**, respectively). Interestingly, the emission energy blue-shifts by nearly the same amount from the unprotonated to the protonated bromide adduct (647 and 587 nm, **2** and **2P**, respectively, 1600 cm^{-1}). $^{31}P\{^1H\}$ NMR studies (downfield shift by ca. 1 ppm in acidic pH) indicate a reduced softness of the P donor ligand

(19) (a) Patterson, H. H.; Roper, G.; Biscoe, J.; Ludi, A.; Blom, N. *J. Lumin.* **1984**, *31/32*, 555. (b) Markert, J. T.; Blom, N.; Roper, G.; Perregaux, A. D.; Nagasundaram, N.; Corson, M. R.; Ludi, A.; Nagle, J. K.; Patterson, H. H. *Chem. Phys. Lett.* **1985**, *118*, 258. (c) Assefa, Z.; DeStefano, F.; Garepapaghi, M.; LaCasce, J., Jr.; Ouellete, S.; Corson, M.; Nagle, J.; Patterson, H. H. *Inorg. Chem.* **1991**, *30*, 2868. (d) Nagle, J.; LaCasce, J., Jr.; Corson, M.; Dolan, P. J., Jr.; Assefa, Z.; Patterson, H. H. *Mol. Cryst. Liq. Cryst.* **1990**, *181*, 356. (e) Assefa, Z.; Shankle, G.; Patterson, H. H.; Reynolds, R. *Inorg. Chem.* **1994**, *33*, 2187.

(20) *Atomic Energy Levels, Circular 467*; Moore, C. E., Ed.; U.S. Department of Commerce, Natioanl Bureau of Standards: Washington, DC, 1958; Vol. 3, p 190.

(21) Ferraudi, G. J. *Elements of Inorganic Photochemistry*; John Wiley & Sons; New York, 1988.

(22) Roundhill, D. M. *Photochemistry and Photophysics of Metal Complexes*; Plenum Press: New York, 1994. An up-to-date overview of luminescence in gold compounds can be found here.

upon protonation. One concludes that this result is consistent with Pyykkö's prediction in that a reduced softness of the phosphorus ligand causes an increase in the Au···Au distance. However, protonation also places a positive charge on each $[(TPAH)AuCl]^+$ center. While the charge probably is centered on the TPA ligand, intermolecular charge repulsion presumably contributes to the lengthening of the Au···Au bond. The charge also influences the chemical shift of the ^{31}P signal. The very short Au···Au distance observed in **4**, 2.92Å, presumably reflects the cation−anion character of the molecule.

Temperature variation is another factor that can affect the Au···Au distance in these complexes. In all of the compounds studied, the Au···Au distance increases slightly with a temperature increase. The Au···Au separation in the protonated compound **1P** increases by ca. 0.019 Å with a temperature increase from 200 to 298 K, and in **2**, the distance changes by ca. 0.02 Å (Table 2). The subsequent blue shift in the emission energy with a temperature increase (from 78 to 298 K) is ca. 700 cm^{-1} for **1**, 400 cm^{-1} for **1P**, 560 cm^{-1} for **2**, and ca. 100 cm^{-1} for **4**.

The LE band energy in the unprotonated, **1**, and protonated, **1P**, chloride complexes has been found to be sensitive to the Au···Au separation and follow roughly the relationship (1),

$$(E + P_i)/r = C \quad (1)$$

where E is the emission energy, r is the distance of Au···Au separation, P is the singlet−triplet energy separation, and C is a constant.[10]

For the free Au(I) ion, the value of P for the separation between the $^1D_2$ and the lowest energy ^3D level is 14 581 cm^{-1}. In the previous study of **1** and **1P**, it was found that a value for P_{Cl} of 12 000cm^{-1} gives a good fit to the structural data. This number happens to be the separation energy between the singlet and triplet states in the Au(I) ion which have the same spin−orbit multiplicity. Using this number for data at 200 K, C becomes 8810 cm^{-1}/Å. For the heavier halides one must assume that the singlet−triplet energy separation decreases, as expected from spin−orbit effects associated with the heavier atoms. Assuming that the change in P_i is the primary cause for the emission energy difference between **1** and **2** (the Au···Au distance is the nearly constant), P_{Br} becomes 11 530 cm^{-1}, a reasonable decrease in the singlet−triplet energy on going from Cl to Br. This suggests further that the Au···Au separation should be approximately 3.24 Å for the protonated species, **2P**, on the basis of the observation that the emission for the protonated species at 587 nm (200 K). A further reduction in the value of P_I to about 10 420 cm^{-1} is suggested for **4** at the observed Au···Au separation of 2.916 Å and an emission energy of 15 267 cm^{-1}. Using this P_I for **3**, the Au···Au distance should be very close to 3.02 Å.

While the roughly linear relationship between the Au···Au separation and the singlet-singlet energy ($E + P_i$), the HOMO−LUMO separation, is suggested both experimentally and theoretically[10] for these weakly interacting species, the internal consistency of these results shows that *both the Au···Au separation distance and the spin−orbit effects are important in determining the emission energies.* Furthermore, the observed reduction in the lifetimes of the ^3MC states on going from Cl to Br to I is a result of the increased spin−orbit contributions of the heavier atoms to the emissions.

While for a given halide ligand X, the Au···Au separation appears to show a direct correlation with the LE emission, a more complicated situation clearly exists for this MC transition when the different halide complexes were compared. For the chloride adduct, **1**, compared to the bromide adduct **2**, the emission energy *blue*-shifts by 620 cm^{-1} (**2** emits at the higher energy) even though the Au···Au distance, as predicted by Pyykkö, has decreased slightly (Table 2). Similarly, the emission energy *blue*-shifts by 752 cm^{-1} on going from **2** to **3** even though a shorter Au···Au distance and, thus, a reduced HOMO-LUMO gap are anticipated for **3**. Thus a comparison of the three compounds, **1**−**3**, indicates that the emission energy increases when the Au···Au distance decreases upon changing the halide ligand. However, for the same X the Au···Au distance and the emission energy increase or decrease together.

These observations appear to imply that an inconsistency exists in the relationship between the Au···Au distance and emission energy as reported earlier for the (TPA)AuCl system. However, the excited state for the gold(I) arises from a d^9s configuration,[20] $^1D_2$ in the ion, which must be split by the ligand field of the phosphine and halide ligands in the order $Cl^- > Br^- > I^-$. Assuming that the MC emission arises from a triplet state in the ^3D manifold of the ion, the blue shift in going from Cl^- to I^- may simply reflect the decreased ^3D ligand field splitting of the long-lived excited state. Apparently this excited state splitting is greater than the diminished separation expected between the ion ^1S and ^1D states with the ligand changes (nephelauxetic effect) or the shortened Au···Au distance as one varies the X ligand.

An emission energy order for the MC transition $I^- > Br^- > Cl^-$ could also be explained by a diminished singlet−triplet separation (splitting, $I^- < Br^- < Cl^-$) in the excited state, ignoring any ligand field splitting. The origin of such an effect in the excited state is unclear, however, and seems to be without precedent and opposite to what is expected from spin−orbit effects.

Nature of the HE Emission Band. A very interesting feature of the photophysical behavior of compounds **2** and **3** is that, under all conditions investigated, the HE and LE emissions appear to operate independently and show substantially different excitation spectra. Such an observation for a single compound is rare and at first tempts one to attribute the two emissions to the presence of two different chemical species. However, the data were reproduced on X-ray-quality single crystals, one of which was used for structural determination purposes. The presence of two different emitting species is, thus, ruled out. Compound **3** also behaves similarly.

When **2** and **3** are excited at 340 nm or longer wavelength, only the HE emission band is observed at both 78 and 298 K. The LE emission is observed only after exciting the sample at 320 nm or shorter wavelength. Thus, each of the two emission bands displays a distinct excitation spectrum, which indicates poor coupling between the emitting states. The profiles of the excitation spectra of the two bands remain the same when the temperature is increased from 78 to 298 K.

Multiple-State Emission from Compounds 2 and 3. The excitation studies clearly indicate that the two (HE and LE) emitting states are thermally nonequilibrated and that they are populated only by direct excitation. The electronic structure is depicted schematically in Figure 10. Excitation at 340 nm to the ES_1 excited state results in the observance of emission originating from the HE excited state. When the excitation is changed to higher energies, e.g. 320 nm or less, excited state ES_2 is populated. Fast thermal quenching then leads the excitation to reside on the LE emitting state. The luminescence data indicate that the thermal quenching rate constant k_2 is much larger than k_1 as no emission has been observed from the ES_1 state when the sample is excited at energies higher than 320 nm. The Stokes shift between the excitation and the LE emission is very large ($>1.6 \times 10^4$) and indicates that a

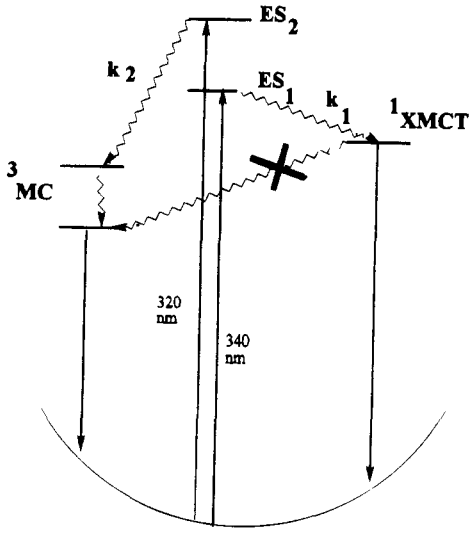

Figure 10. Schematic drawing describing the nature of the various excited states leading to emission in compounds **2** and **3**.

significant geometrical distortion exists with this excitation. As the LE band has been correlated with the Au···Au interaction,[10] the large distortion may indicate a shortening of the M−M separation and bond formation in the excited state. Excitation from the metal-centered antibonding σ_u HOMO can reduce the Au···Au separation and cause a large geometrical change between the ground singlet and excited triplet states.

The HE emission band has been observed for the bromide, **2**, and iodide, **3**, adducts while it is absent for the chloride species, **1**. For both **2** and **3**, the HE band has a structured nature with an average spacing for the vibronic components of 350−500 cm^{-1}. The vibronic band is probably associated with metal−ligand stretching frequencies. The fact that the vibronic spacing decreases from the bromide to the iodide adduct (**2** and **3**, respectively) is consistent, at least qualitatively, with a reduction in the metal−ligand bond strength and/or an increased mass in going from Br^- to I^-. However, Au−X, X = Br^-, I^-, vibrations generally appear around 200−330 cm^{-1}. The Au−P stretching mode of the phosphine ligand would be expected to appear at somewhat higher energy, and indeed, the vibronic structure observed may reflect both gold−halide and gold−phosphine vibrational modes. The vibronic structure was observed only in the emission and not in the excitation spectra. The orbital parentages in the ground state may be different from those of the excited state. On the basis of these observations, the HE emission band is assigned to a band originating from a ligand to metal (largely halide) charge transfer (XMCT) excitation.

The fact that the HE band is absent in spectra of the chloride products but present in those of the bromide and iodide complexes is consistent with the charge transfer transition assignment. The ease of oxidation and by inference the σ-donating ability increase on going from chloride to bromide and to the iodide, thus influencing the LMCT excitations to ES_1.

The EH molecular orbital calculation is also consistent with this proposed assignment of the HE emission. The HOMO of (TPA)AuCl consists of largely a metal $5d_{z^2}$ and 6s contribution along with $3p_z$ contribution from the P atom of the TPA ligand.[10] The metal contribution in the HOMO decreases when Cl^- is replaced by Br^- and then I^-. For **3**, the HOMO consists of a large contribution from the iodide $6p_z$ orbital. The SHOMO of **3** consists of largely an iodide contribution. On the other hand, the LUMO of all the complexes consists of a large contribution form the metal $6p_z$ orbital. The EH data indicate that the lowest transitions in (TPA)AuCl correspond to a metal-centered transition. In the presence of iodide, the lowest transitions consist of a large XMCT character. The short lifetime (in the nanosecond range, Table 3) of the HE band supports our assignment of the emission to a ^{1}XMCT fluorescence.

Conclusions. In this paper, temperature-dependent PL and crystallographic studies of the crossed dimerized TPA−gold(I) compounds are reported. Compounds **1**−**4** all show an intense LE metal-centered red emission at low temperatures. The auriophilic Au···Au interaction is suggested as the source for this visible emission. The Au···Au distance is influenced by several factors, including protonation of the TPA ligand, temperature, and ligand X variations which shift the emission energy. The blue shifts observed in **1** and **2** as a result of protonation correspond to ca. 1900 and 1600 cm^{-1}, respectively. Less pronounced blue shifts are observed with a temperature increase. A maximum shift (between 78 and 298 K) of 700 cm^{-1} has been observed for **1**. In addition, the LE emission band blue-shifts as the halide X is changed from Cl to Br to I. Compounds **2** and **3** show a structured HE white emission when excited at 340 nm. The HE emission band has an excitation profile distinctively different from that of the LE band. No coupling between these two excited states has been observed. The lifetime of the HE emission band is in nanosecond region as opposed to the microsecond value observed for the LE band. On the basis of these PL studies, compounds **2** and **3** are believed to show multiple-state emission originating from thermally nonequilibrated excited states having different orbital parentages. The HE emission band is determined to originate from the singlet halide to metal CT excited state (^{1}XMCT) while the LE emission arises from a metal-centered triplet excited state ^{3}MC.

Acknowledgment. The support of the National Science Foundation, Grant CHE-9300107, the Welch Foundation, and the Texas Advanced Research Program is gratefully acknowledged.

Supporting Information Available: For complex **1**, a discussion of the crystallographic experimental details and tables of crystallographic data, hydrogen coordinates, thermal parameters, and bond distances and angles (10 pages). Ordering information is given on any current masthead page. Tables of F_o and $\sigma(F')$ (7 pages) are available from J.P.F. upon request.

IC950254Z